All-optical switching using nonlinear subwavelength Mach-Zehnder on silicon

Ivan Glesk,[1] Przemek J. Bock,[3] Pavel Cheben,[2] Jens H. Schmid,[2] Jean Lapointe,[2] and Siegfried Janz[2]

[1]*Department of Electronic and Electrical Engineering, University of Strathclyde, Glasgow, United Kingdom*
[2]*Institute for Microstructural Sciences, National Research Council Canada, Ottawa, Canada*
[3]*Centre for Research in Photonics, University of Ottawa, Ottawa, Canada*
ivan.glesk@eee.strath.ac.uk

Abstract: We report on the experimental demonstration of ultrafast all-optical switching and wavelength down-conversion based on a novel nonlinear Mach-Zehnder interferometer with subwavelength grating and wire waveguides. Unlike other periodic waveguides such as line-defects in a 2D photonic crystal lattice, a subwavelength grating waveguide confines the light as a conventional index-guided structure and does not exhibit optically resonant behaviour. Since the device had no dedicated port to input optical signal to control switching a new approach was also implemented for all-optical switching control.

OCIS codes: (130.3120) Integrated optics devices; (050.1950) Diffraction gratings; (050.6624) Subwavelength structures, (130.4815) All-optical switching devices.

References and links

[1] J. Leuthold, C. Koos, and W. Freude, "Nonlinear silicon photonics," Nature Photonics **4**, 535-544 (2010).

[2] A. Densmore, D.-X. Xu, P. Waldron, S. Janz, P. Cheben, J. Lapointe, A. Delage, B. Lamontagne, J. H. Schmid, and E. Post, "A silicon-on-insulator photonic wire based evanescent field sensor," IEEE Photon. Tech. Lett. **18**, 2520–2522 (2006).

[3] L. K. Oxenløwe, F. G. Agis, C. Ware, S. Kurimura, H. C. H. Mulvad, M. Galili, K. Kitamura, H. Nakajima, J. Ichikawa, D. Erasme, A. T. Clausen, and P. Jeppesen, "640 Gbit/s clock recovery using periodically poled lithium niobate," Electron. Lett. **44**, 370-371 (2008).

[4] S. J. Madden, D. Y. Choi, D. A. Bulla, A. V. Rode, B. Luther-Davies, V. G. Ta'eed, M. D. Pelusi, and B. J. Eggleton, "Long, low loss etched As_2S_3 chalcogenide waveguides for all-optical signal regeneration," Opt. Express **15**, 14414-14421 (2007).

[5] F. Parmigiani, S. Asimakis, N. Sugimoto, F. Koizumi, P. Petropoulos, and D. J. Richardson, "2R regenerator based on a 2-m-long highly nonlinear bismuth oxide fiber," Opt. Express **14**, 5038-5044 (2006).

[6] J. M. Hales and J. W. Perry, *Introduction to Organic Electronic and Optoelectronic Materials and Device* (eds S.-S. Sun and L. Dalton) 521–579 (CRC, 2008).

[7] S. Fischer, M. Duelk, M. Puleo, R. Girardi, E. Gamper, W. Vogt, W. Hunziker, E. Gini; and H. Melchior, "40-Gb/s OTDM to 4x10 Gb/s WDM conversion in monolithic InP Mach-Zehnder interferometer module," IEEE Photon. Tech. Lett. **11**, 1262-1264 (1999).

[8] M. Eiselt, "Optical loop mirror with semiconductor-laser amplifier," Electron. Lett. **28**, 1509 (1992.

[9] J. P. Sokoloff, P. R. Prucnal, I. Glesk, and M. Kane, "A Terahertz Optical Asymmetric Demultiplexer (TOAD)," IEEE Photon. Technol. Lett. **5**, 787-790 (1993).

[10] N. S. Patel, K. A. Rauschenbach, and K. L. Hall, "40 Gb/s demultiplexing using an ultrafast nonlinear interferometer," IEEE Photon. Technol. Lett. **8**, 1695 (1996).

[11] N. J. Doran and D. Wood, "Nonlinear-optical loop mirror," Opt. Lett. **13**, 56 (1988).

[12] K. Kravtsov, P. R. Prucnal, and M. M. Bubnov, "Simple nonlinear interferometer-based all-optical thresholder and its applications for optical CDMA," Opt. Express **15**, 13114–13122 (2007).

[13] M. P. Fok and C. Shu, "Highly Nonlinear Bismuth-Oxide Fiber Based Dispersion Imbalanced Loop Mirror for Interferometric Noise Suppression," in *Optical Fiber Communication Conference and Exposition and The National Fiber Optic Engineers Conference*, OSA Technical Digest (CD) (Optical Society of America, 2008), paper OThJ5.

[14] V. G. Ta'eed, L. Fu, M. Pelusi, M. Rochette, I. C. Littler, D. J. Moss, and B. J. Eggleton, "Error free all optical wavelength conversion in highly nonlinear As-Se chalcogenide glass fiber," Opt. Express **14**, 10371–10376 (2006).

[15] M. Rochette, L. B. Fu, V. G. Ta'eed, I. C. M. Littler, D. J. Moss, and B. J. Eggleton, "2R optical regeneration: Beyond noise compression to BER reduction," IEEE J. Sel. Top. Quant. Electron. Special Issue on All-Optical Signal Processing **12**, 736 (2006).

[16] M. R. E. Lamont, V. G. Ta'eed, M. A. F. Roelens, D. J. Moss, B. J. Eggleton, D. Choy, S. Madden, and B. Luther-Davies, "Error-free wavelength conversion via cross phase modulation in 5 cm of As2S3 chalcogenide glass rib waveguide," Electron. Lett. **43**, 945 (2007).

[17] D. I. Yeom, E. C. Mägi, M. R. E. Lamont, M. A. F. Roelens, L. Fu, and B. J. Eggleton, "Low-threshold supercontinuum generation in highly nonlinear chalcogenide nanowires," Opt. Lett. **33**, 660–662 (2008).

[18] M. D. Pelusi, F. Luan, E. Magi, M. R. E. Lamont, D. J. Moss, B. J. Eggleton, J. S. Sanghera, L. B. Shaw, and I. D. Aggarwal, "High bit rate all-optical signal processing in a fiber photonic wire," Opt. Express **16**, 11506–11512 (2008).

[19] R. Salem, M. A. Foster, A. C. Turner, D. F. Geraghty, M. Lipson, and A. L. Gaeta, "Signal regeneration using low-power four-wave mixing on silicon chip," Nat. Photonics **2**, 35–38 (2008).

[20] B. G. Lee, A. Biberman, A. C. Turner-Foster, M. A. Foster, M. Lipson, A. L. Gaeta, and K. Bergman," Demonstration of broadband wavelength conversion at 40 Gb/s in silicon waveguides," IEEE Photon. Technol. Lett. **21**, 182–184 (2009).

[21] F. A. M. Melloni, A. Canciamilla, C. Ferrari, and M. Torregiani, "Phase preserving wavelength conversion over 6Thz in a silicon coupled resonator optical waveguide", in *Optical Fiber Communication Conference*, Post deadline Paper of 2009 OSA Technical Digest Series (Optical Society of America, 2009), paper PDPA6.

[22] Y. Vlasov, W. M. J. Green, and F. Xia, "High-throughput silicon nanophotonic wavelength-insensitive switch for on-chip optical networks," Nat. Photonics **2**, 242–246 (2008).

[23] B. Jalali, D. R. Solli, and S. Gupta, "Silicon's time lens," Nat. Photonics **3**, 8–10 (2009).

[24] M. D. Pelusi, V. G. Ta'eed, M. R. E. Lamont, S. Madden, D. Y. Choi, B. Luther-Davies, and B. J. Eggleton, "Ultra-high Nonlinear As_2S_3 planar waveguide for 160-Gb/s optical time-division demultiplexing by four-wave mixing," IEEE Photon. Technol. Lett. **19**, 1496–1498 (2007).

[25] P. Cheben, P. J. Bock, J. H. Schmid, J. Lapointe, S. Janz, D.-X. Xu, A. Densmore, A. Delâge, B. Lamontagne and T. J. Hall, "Refractive index engineering with subwavelength gratings for efficient microphotonic couplers and planar waveguide multiplexers," Opt. Lett. **35**, 2526-2528 (2010).

[26] Y. A. Vlasov, M. O'Boyle, H. F. Hamann, and S. J. McNab, "Active control of slow light on a chip with photonic crystal waveguides," Nature **438**, 65-69 (2005).

[27] http://ab-initio.mit.edu/wiki/index.php/MIT_Photonic_Bands.

[28] P. J. Bock, P. Cheben, J. H. Schmid, J. Lapointe, A. Delâge, S. Janz, G. C. Aers, D.-X. Xu, A. Densmore, and T. J. Hall, "Subwavelength grating periodic structures in silicon-on-insulator: a new type of microphotonic waveguide," Opt. Express **18**, 20251-20262 (2010).

[29] R. Akimoto, S. Gozu, T. Mozume, and H. Ishikawa, "Monolithically Integrated Ultrafast All-Optical Switch Consisting of Intersubband Optical Nonlinear Waveguide and Michelson Interferometer," in *Conference on Lasers and Electro-Optics/Quantum Electronics and Laser Science and Photonic Applications Systems Technologies*, Technical Digest (CD) (Optical Society of America, 2011), paper CTuW2.

1. Introduction

To be able to sustain future needs of rapidly growing data traffic we will need new technological innovations. This task is becoming more and more challenging with data rates exceeding not so long ago the unthinkable 100 Gbit/s. With these advances our ability for a "bit by bit" data processing is quickly disappearing. The reason is the electronic bottleneck. The electronic bottleneck is not something new if looking back into the history of data communication but we have been always able to overcome its limitations thanks to inventions which include such discoveries as vacuum tubes, Si-based electronics, CMOS integration, GaAs technology. Unfortunately the electronic bottleneck we face today has more fundamental roots. The consensus seems to be that the electronics as is known to us today may not be able to deliver switching speeds we will need and innovative solutions will be required. In the past two plus decades to address telecom needs in the area of fast switching, routing and signal processing the research has been focused on optical approaches to such functionalities in the electronic domain. Historically, significant progress has been recorded in several areas leading to optical amplifiers, MEMS, all-optical signal regeneration including wavelength conversion, just to name a few.

In spite of the inherent ability of the optical fiber to carry tremendous amounts of data, the optical serial data has always been limited by the speed of the electronic data processing,

routing and switching at the moment commercially available. These limitations are often due to the fact that optical data have to be first converted into the electronic domain before switching or routing can be carried out. The process of opto-electro-opto (OEO) conversion thereby creates a barrier as most electronic components available today are not able to match the optical data rates available or supported by the optical fiber. In order to eliminate the electronic bottleneck we need solutions that are capable of processing optical data preferably without any OEO conversion.

Before going any further for the purpose of this article, let us first focus on a terminology related to optical signal processing, namely the use of the terms optical switching and all-optical switching. Both terms are often used loosely although there is a fundamental difference between the approaches they describe.

By optical switching we understand cases where a light wave carrying optical data is controlled by a signal which is NOT optical (RF, heat, etc.).

In the case of all-optical switching the routing of photonic data is controlled by the signal in its optical form – here literally "light controls light." This control can happen through nonlinear interactions between both optical signals in optical material of "our choice." An excellent overview of such interactions was given in [1]. Since no electronics is involved nor is needed to execute such switching/routing, the electronic bottleneck does not apply here. Many demonstrated concepts already surpassed capabilities of current electronics. Materials including silicon [2], periodically pulled Lithium Niobate [3], chalcogenide glass [4], passive/ active semiconductors [5], different types of optical fibers, even silicon–organic hybrid (SOH) approach taking advantage of the organic nonlinear materials that have large Kerr coefficients [6] have been investigated for their usability to support ultrahigh speed all-optical switching.
Generally non-linear (NL) materials used in all-optical switching applications belong to two categories - exhibiting active or exhibiting passive nonlinearity. A good example of the active optical nonlinearity is the DC biased semiconductor optical amplifier (SOA). Biased SOAs offer very strong resonant type non-linearity. The NL onset can be very fast (< 1ps) but the drawback in the SOA gain recovery dynamics (ranging anywhere between few to hundreds of ps) which usually sets an upper limit on the maximum switching speed. It can also introduce undesired bit pattern effects. Both effects have been very extensively investigated to improve the performance of Mach-Zehnder SOA-based switching devices [7], Semiconductor Laser Amplifier in a Loop Mirror (SLALOM) [8], Terahertz Optical Asymmetric Demultiplexer (TOAD) [9], and Ultra-fast Nonlinear Interferometer (UNI) [10]. On the other hand, since biased SOAs can offer optical gain to the passing signal the switched output can be amplified which is a very attractive feature of this type of all-optical switching devices. Commercially available SOAs with low saturation switching energy and 10 ps record low gain recovery time were reported by The Center for Integrated Photonics, Ltd. (CIP Technologies) in 2007.

The use of a passive nonlinearity to demonstrate all-optical switching was exploited by Doran and Wood [11] in experiments with a Sagnac interferometer also called Nonlinear Optical Loop Mirror (NOLM). Because of a weak nonlinear coefficient the interaction length to observe complete switching had to be l = 15 km. Following this concept and to shorten the interaction length, first polarization maintaining (PM) fiber, later Bismuth oxide then Germanium oxide fiber were used for the NOLM, thus shortening the NOLM loop from a few hundred (case of PM) to just a few meters [12,13], respectively.

To demonstrate all-optical switching, also other types of optical interferometers including Mach-Zehnder interferometer (MZI) were investigated. In contrary to Sagnac, a MZI is a two-arm interferometer which requires temperature stabilization. If it is not stabilized it will act as a sensor rather than a stable switching device. Such stabilization can be achieved via device integration. However, integration puts practical restrictions on the MZI arms length, and shortens the available length l for interaction. With this limitation we need a NL material with high enough second-order non-linear index n_2 (order of ~6×10^{-18} m^2/W or greater [1]) which will deliver the required π phase shift for achieving complete switching at the device output. In recent years a significant progress has been made in the search for materials offering high nonlinear parameter $\gamma = 2\pi n_2 / (\lambda A_{eff})$, where A_{eff} is the effective interaction area. A specially

silicon and chalcogenide waveguides have achieved unusually high γ's ranging from 1.2 W^{-1} m^{-1} in chalcogenide fiber [14], 15 W^{-1} m^{-1} in ChG waveguides [15,16], to 95 W^{-1} m^{-1} in ChG tapered fiber nanowires [17], to 300 W^{-1} m^{-1} in Si nanowires [18]. Also very impressive demonstrations of all-optical signal processing in silicon devices have been reported [19-24].

In this paper to the best of our knowledge we demonstrate for the first time a practical realization of a novel ultra-fast all-optical interferometric sampling/switching device based on photonic nanowire and subwavelength grating *waveguides* placed in the Mach-Zehnder geometry capable of all-optical picosecond sampling and switching.

2. Design and fabrication

The schematic diagram of the device is shown in Fig. 1. The device was fabricated as follows. Its one arm is comprised of a 50 μm SWG taper [25], followed by a SWG straight waveguide (Λ = 400 nm, w = 300 nm, duty cycle 50%) with a maximum length L = 4580 μm and an identical SWG taper to transition back to wire waveguide as schematically shown in Fig. 1. The second arm is comprised of a wire waveguide (450 × 260 nm^2) with two 50 μm SWG tapers back-to-back to compensate for the SWG tapers in the signal arm. The MZI uses a 50:50 y-splitter implemented with two 75-μm-long and 15-μm-wide s-bends.

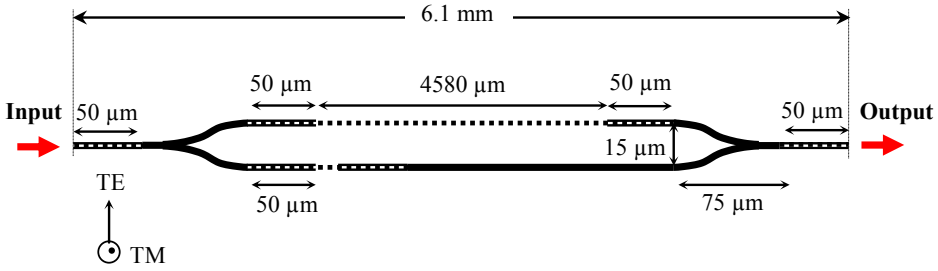

Fig. 1. Schematic of the Mach-Zehnder interferometer (MZI). The MZI signal arm is comprised of a 50 μm SWG taper followed by a SWG waveguide (Λ = 400 nm, w = 300 nm, duty cycle 50%, length L = 4580 μm) and a SWG taper to transition back to wire waveguide. The reference arm is a wire waveguide (450 × 260 nm^2) with a taper-to-taper structure (two 50 μm SWG tapers) to equalize the loss of both arms.

This structure was fabricated using commercially available SOI substrates with a 0.26 μm thick silicon layer and 2 μm thick buried oxide (BOX). Electron beam lithography was used to define the waveguide layout in high contrast hydrogen silsesquioxane resist, which formed SiO_2 upon electron beam exposure. We used inductively coupled plasma reactive ion etching (ICP-RIE) to transfer the waveguide pattern onto the silicon layer. Samples were coated with a 2 μm thick polymer (SU-8, n ~ 1.577 at λ = 1.55 μm), then cleaved into separate chips and facets polished using a standard lapping and polishing machine using a chuck holding stacks of samples with the facets towards the polishing plate.

Figure 2 shows scanning electron microscope (SEM) images of the fabricated structures including a SWG taper (Fig. 2(a)), an optical microscope image of a MZI with SEM image detail of the SWG straight waveguide and the wire waveguide. From the SEM images it was determined that a fabrication bias of 50 nm was present. Therefore the actual dimensions of the SWG are Λ = 400 nm and w = 250 nm with a duty cycle of 38%. Actual wire waveguide width is 400 nm.

The group index of a SWG straight waveguide was measured interferometrically for λ = 1480 nm – 1580 nm using the same tuneable external cavity semiconductor laser. Group index was calculated using $n_g^{SWG} = \lambda_{min}\lambda_{max}/[2L(\lambda_{min} - \lambda_{max})] + n_g^{wire}$, where λ_{min} and λ_{max} are the wavelengths at the minimum and maximum intensities of the interference fringes in the MZI transmission spectrum, L = 4580 μm is the length of the SWG straight waveguide and

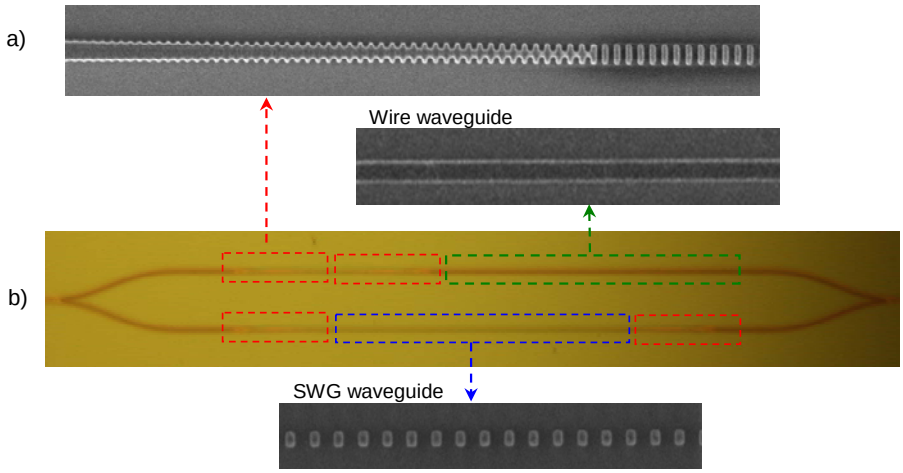

Fig. 2. Scanning electron microscope (SEM) images of fabricated structures including: a) SWG taper b) Optical microscope image of a MZI (L = 150 μm) with SEM image detail of the SWG arm and the reference arm (wire waveguide). Interferometric measurements were done with a MZI with a 4580 μm long SWG waveguide.

n_g^{wire} is the group index of the wire waveguide [26]. The wire waveguide group index was found by using a mode solver (we used commercial software purchased from Optiwave Corp.) to calculate the wavelength-dependent effective index of a 400 × 260 nm^2 waveguide with silicon core and SU-8 cladding on a silica substrate for λ = 1480 nm – 1580 nm. The wire waveguide group index is found to be nearly constant across the wavelength range, with values of n_g^{TE} ~ 4.1 and n_g^{TM} ~ 4.2. The interferometrically measured group index of SWG straight waveguide is presented in Fig. 3 and is compared to the theoretically

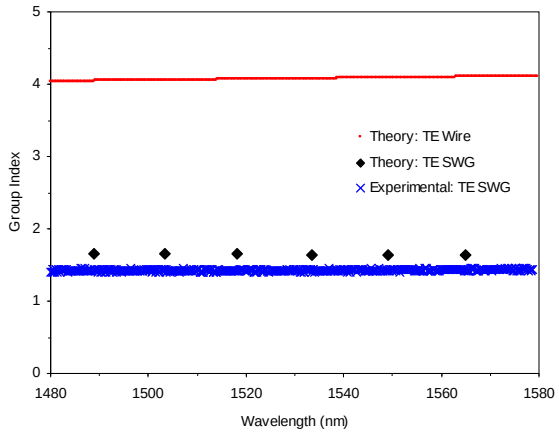

Fig. 3. The measured group index for a SWG waveguide using a Si wire waveguide reference arm and a 4580 μm long SWG straight waveguide signal arm. The group index of the reference wire waveguide (red) is estimated using a mode solver (Optiwave Corp.) by calculating the effective index of a 400 × 260 nm^2 waveguide with silicon core, SU-8 upper cladding and SiO_2 bottom cladding. The calculated (black) and the interferometrically measured (blue) group index for the SWG waveguide are shown for comparison.

calculated (MPB, [27]) group index for a periodic waveguide with the dimensions as measured by SEM, i.e. 38 % duty cycle. The agreement between experiment and theory is excellent and is consistent with our previous results [28], indicating a low and nearly constant group index of n_g~1.5 over the measured wavelength range.

3. Demonstration of ultrafast all-optical switching and wavelength conversion

Now the concept of the device switching operation will be explained. The manufactured Mach-Zehnder all-optical interferometric switch (MZIS) is a two port all-optical device

with one input and one output port. It has no dedicated port for the optical clock (pump) injection to control its all-optical switching operation. Therefore, we developed a new technique for implementing the all-optical switching control of the MZIS. We realized that the all-optical control can be done via all-optically invoked ultrafast self switching by exploiting the uneven optical power densities per-unit-volume of optical clock (pump) pulses when they propagate in MZIS arms. Note one MZIS arm is a wire waveguide and the second is a SWG waveguide. The ratio of optical power densities for this MZIS can be easily estimated. First the software purchased from Optiwave Corp. was used to calculate the confinement factor of the SWG waveguide (at the center of the Si segment) and then the wire waveguide. We found that the ratio of confinement factors per-core-unit-volume is approximately $(\Gamma_w/V_w)/(\Gamma_{swg}/V_{swg}) \sim 15$, where Γ_w and Γ_{swg} are the wire and SWG waveguide confinement factors and V_w and V_{swg} are wire and SWG waveguide volumes, respectively. This indicates that the optical power density in the wire waveguide is ~15 times greater than that of the SWG waveguide. Now if the proper conditions are met [1], and sufficient level of the optical clock peak power is delivered to the MZIS input, the nonlinear index change triggered inside the wire waveguide will be larger than in the SWG waveguide. This will induce a relative phase change between both arms of the MZIS which will be experienced by the optical probe signal (cw or low power data pulses) immediately following such high peak power optical clock. If the phase difference equals π, complete switching is achieved at the MZIS output. If not, incomplete switching will be observed. However, in order to satisfy interferometric conditions at the device output the use of optical pulses as the probe signal would also require both of the MZIS arms to be of equal optical length. Since in our experimentation with the MZIS device this was not fulfilled, we used cw laser light as the optical probe and the pump probe technique as a method for the demonstration of ultrafast picosecond all-optical switching capabilities of this novel interferometric structure. Our approach is conceptually illustrated in Fig. 4.

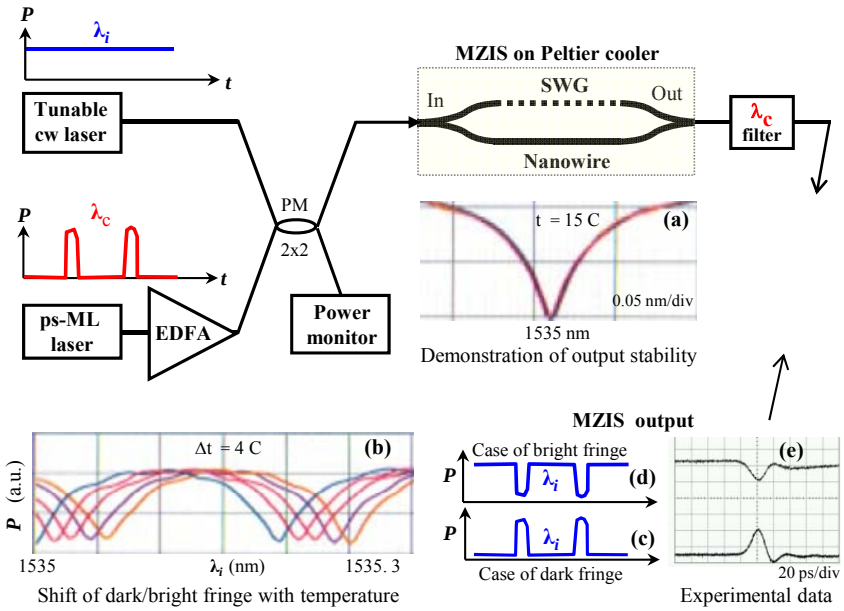

Fig. 4. Schematic diagram illustrating the concept used to demonstrate ultrafast all-optical sampling/switching capabilities of a fabricated device. A TEC cooler keeps the Mach-Zehnder all-optical switch at a constant temperature -inset (a). Temperature was used to select interferometric conditions (dark or bright fringe) at the MZIS output –inset (b). Optical clock was applied to invoke all-optical sampling/switching -insets (c) and (d); (e) -experimental results showing 1 ps pulses as seen on the bandwidth limited oscilloscope.

Because the MZIS is an interferometric device its constant temperature was assured by device temperature stabilization with a Peltier cooler. It was experimentally confirmed that such stabilization was sufficient as seen in Fig. 4(a) which is an overlay image of multiple wavelength scans of the MZIS output around a bright interferometric fringe taken at 15°C.

It confirms excellent device temperature stability but its operation is not restricted to thermal stability at 15°C and this is not the only operating point of the device which will be evident from experimental results shown bellow. Device temperature tuning was then used to select either a bright or a dark fringe at the MZIS output for the selected probe wavelength λ_i - see Fig. 4(b) for the illustration. Depending on the selected interferometric condition (dark or bright fringe) the corresponding scenario depicted in Fig. 4(c) or Fig. 4(d) was observed after a high peak power optical clock/pump was applied. As for the optical probe signal we used a 6 dBm cw external cavity tuneable semiconductor laser set to λ_i = 1535.04 nm. For the optical pump/clock to all-optically control the MZIS switching operation we used one of the two Erbium doped fiber mode locked lasers at λ_c = 1558 nm by the method discussed below. The experimental setup to demonstrate ultrafast all-optical switching capabilities of the novel MZIS structure is shown in Fig. 5 and was used to conduct two sets of experiments.

In the first set of experiments the cw probe was coupled by a 2×2 polarization maintaining coupler (splitting ratio 50:50) with optical pump/clock pulses generated by a tuneable passively mode locked Erbium doped fiber laser (EDFL) from PriTel which produced 1 ps full-width at half-maximum (FWHM) optical pulses 1 nm wide at λ_c = 1558 nm and at a repetition rate of 18.54 MHz with an average output power of 0.54 mW (29 W peak) followed by a 30 dBm EDFA with adjustable gain. The combined signal was then coupled in and out of the MZIS chip using a tapered PM fibres (spot size of ~2.5 μm). At the chip output the optical pump/clock was filtered out using a 400 GHz array waveguide grating (AWG). The probe signal at λ_i = 1535.04 nm after passing the AWG was amplified by a signal EDFA and after passing a 2.8 nm optical band pass filter viewed using a sampling oscilloscope with a 30 GHz optical plugin, optical autocorrelator, optical power meter, and OSA, respectively. The inset of Fig. 5 is an overlaid picture taken by the OSA showing the optical spectrum of the mode locked (ML) laser, pump/clock amplifying EDFA, and amplified cw signal at the MZIS output, respectively.

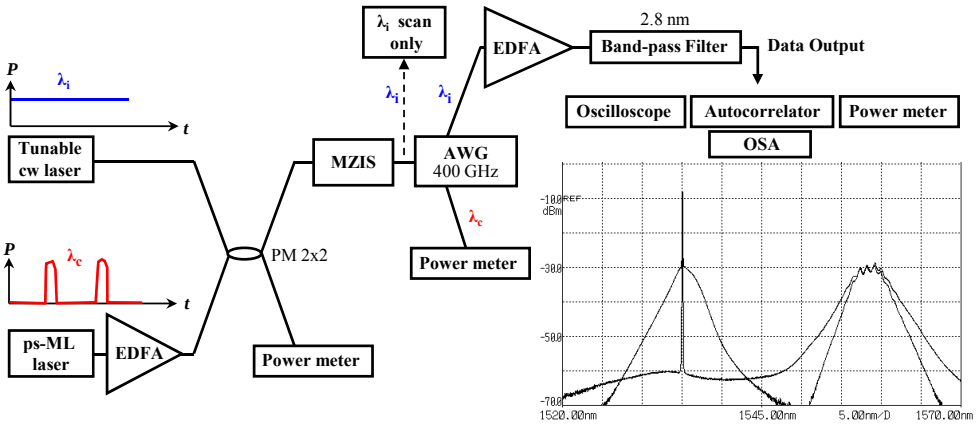

Fig. 5. Schematic diagram of the experimental setup. A tunable continuous wave (cw) external cavity semiconductor laser used as a probe signal at λ_i = 1535.04 nm is coupled by polarization maintaining 2×2 PM coupler with optical pump/clock, a picosecond fiber mode locked laser at λ_c = 1558nm, into a MZIS via a PM tapered fiber. A 400 GHz array waveguide grating (AWG) separates both signals at the MZIS output. The inset is an overlaid picture taken by an OSA showing optical spectrum of the passively ML EDF laser, optical clock amplifying EDFA, and amplified cw signal at the device output, respectively.

The MZIS' all-optical switching capabilities are demonstrated in Fig. 4(e). The experimental results were obtained by closely following the described methodology. Figure 4(e) shows exiting 1 ps optical pulses now at the converted wavelength λ_i = 1535.04 nm as seen by the bandwidth limited oscilloscope via a 30 GHz optical sampling head. To obtain these results (the lower/upper trace in Fig. 4(e) the MZIS was first tuned to a dark/bright fringe, respectively and then high peak power (29 W) optical pump/clock pulse

(1 ps FWHM at λ_c = 1558 nm) with 18.54 MHz repetition rate was applied at the MZIS input.

Figure 6 is the result of follow up experiments showing zoomed images of the MZIS output. Here before applying the optical pump/clock, the MZIS was first temperature tuned to a dark fringe at the output. Figure 6(a) combines three different experimental results: both cw and clock are "ON", clock only "ON", and cw only "ON", respectively.

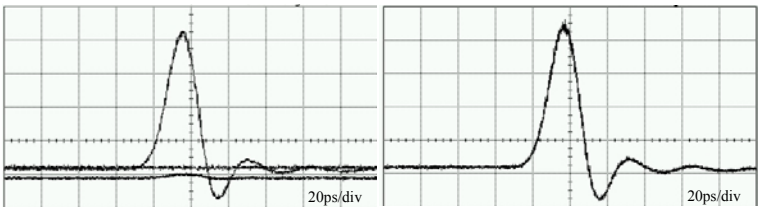

Fig. 6. Amplified switched MZIS output as seen by the bandwidth limited oscilloscope. (a) overlaid picture when both cw and clock are ON, clock ON and cw ON only; (b) - switched output after MZIS was temperature tuned to the next dark fringe.

By the close examination of Fig. 6(a) we can notice a small clock leak (see a small blip on the lowest trace) caused by the insufficient clock filtering at the MZIS output by the used AWG during these experiments.

Figure 6(b) is also the MZIS output when both cw and clock are "ON". However, prior this experiments the MZIS was temperature re-tuned to the adjacent dark fringe. This result confirms very good device temperature stability and its operation at various temperatures.

The demonstrated all-optical picosecond switching shown in Fig. 4 and Fig. 6 is effectively all-optical wavelength down-conversion of 1 ps optical clock pulses with wavelength λ_c = 1558 nm on a new carrier with wavelength λ_i = 1535.04 nm. In our experiments we have not recorded a pulse width change between optical pump/clock pulse at the MZIS input and the wavelength down-converted signal at the MZIS output. A 'slightly wider' resulting gating window (if compared to the pulse width of the pump) attributed to the intersubband carrier relaxation from the exited subband to the ground subband, was reported in [29] in experiments with a monolithically integrated ultrafast intersubband switch utilizing a Michelson interferometer with one of its arm functioning as a nonlinear waveguide using a reflective cross-phase modulation (XPM) effect.

The second set of experiments with the MZIS was carried out at the telecom rate of OC-192. We also used the setup described in Fig. 5. Here a PriTel actively mode locked EDF laser also running at λ_c = 1558 nm and producing 3 ps FWHM 1.2 nm wide optical pulses at OC-192 was used as the optical pump/clock to control the MZIS all-optical switching. The laser average output power of 8.3 mW before used as the optical control was first amplified by a 20 dBm EDFA with adjustable gain, boosting the laser peak power to 3.3 W. Obtained experimental results are shown in Fig. 7. The upper (lower) trace in Fig 7(a) shows the all-

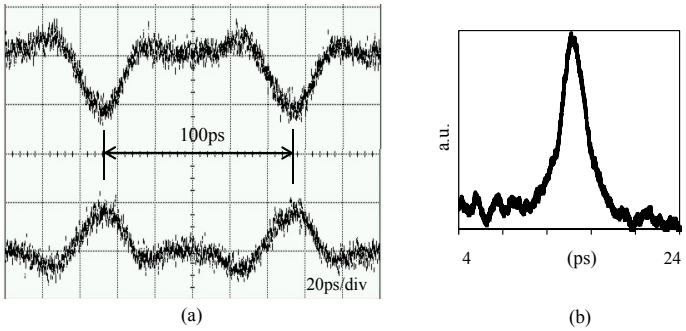

Fig. 7. Amplified MZIS switched output as seen using bandwidth limited oscilloscope. Top trace –the MZIS output when temperature was tuned for the operating point to sit on a bright

fringe; lower trace –the MZIS output tuned to sit on a dark fringe, b) autocorrelation trace of the wavelength switched signal at λ_i = 1535.04 nm.

optically switched/wavelength down-converted ~3 ps pulses at λ_i = 1535.04 nm exiting from the output of the MZIS for the case when the MZIS was first temperature tuned for the operating point to sit at the bright (dark) fringe, respectively before the optical clock/pump at λ_c = 1558 nm was applied. Since, in this set of experiments the available optical pump/clock peak power was approximately 8.8 times lower than the one we used in the first set of our experiments the signal contrast at the MZIS output is lower.

Figure 7(b) is an autocorrelation of the switched/wavelength down-converted output at the wavelength λ_i = 1535.04 nm confirming picosecond all-optical switching capabilities of this novel MZIS switching architecture.

4. Conclusion

We experimentally demonstrated and analysed a novel ultrafast all-optical nonlinear Mach-Zehnder interferometric switching device, the MZIS which is based on the combination of subwavelength grating waveguide and wire waveguide. The device is capable of performing all-optical picosecond switching. We also demonstrated the device capability to perform all-optical wavelength down-conversion of picosecond pulses from 1558 nm to 1535.04 nm at the repetition rates of 18.54 MHz and OC-192. Since the device has no dedicated port to input an optical signal to control its switching operation, a new approach was developed and implemented for all-optical switching control.

5. Acknowledgment

Authors would like to thank to Dr. K. V. Ready the President of PriTel for his generous support and for providing mode the locked lasers and the EDFAs to conduct these experiments.